RSC Advances

ROYAL SOCIETY OF CHEMISTRY

www.rsc.org/advances

Graphic Abstract

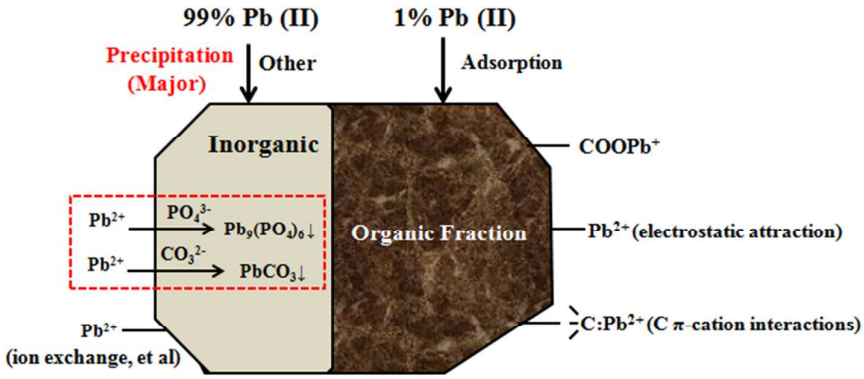

The inorganic fraction of biochar played the dominant role in the Pb(II) removal mainly via inner-sphere complexation and precipitation while the organic carbon sorbed Pb(II) via intrinsic chemical affinity, and/or electrostatic attraction

Cite this: DOI: 10.1039/c0xx00000x

www.rsc.org/xxxxxx

ARTICLE TYPE

Interaction of organic and inorganic fractions of biochar with Pb(II) ion: Further elucidation of mechanisms for Pb(II) removal by biochar

Xiaoyun Xu,[a] Xinde Cao,*[a] Ling Zhao,[a] Haojun Zhou,[a] and Qishi Luo[b]

Received (in XXX, XXX) Xth XXXXXXXXX 20XX, Accepted Xth XXXXXXXXX 20XX

DOI: 10.1039/b000000x

In recent years, many literatures had documented waste biomass-derived biochar as a promising carbonaceous biosorbent for heavy metal removal from aqueous solution and attributed the effective removal to the surface sorption via organic functional groups. This study took the further attempts to elucidate the mechanisms of Pb(II) removal by biochar via separating the organic and inorganic fractions from biochars and investigating their contributions to the Pb(II) removal. Two biochars were prepared from dairy manure and rice straw at 500°C through a pyrolysis process. The sorption capacities of organic fractions in both biochars were only around 1 mg g^{-1}, accounting for 0.4%-0.6% of the Pb(II) removal by the whole biochars, while the inorganic fractions showed sorption capacities of over 300 mg g^{-1}, occupying more than 99% of Pb(II) removal. Sorption of Pb(II) by the organic fraction was probably through electrostatic attraction, intrinsic chemical affinity with $–COO^-$, and/or cation-π interactions, while the inorganic fraction sorbed Pb(II) via the chemisorption, primarily through the inner-sphere complexation and precipitation. XRD analysis and MINTEQ modeling evidenced formation of $PbCO_3$, $Pb_3(CO_3)_2(OH)_2$, and $Pb_5(PO_4)_3Cl$ in the inorganic fractions, among which precipitation with phosphate contributed more to the Pb(II) removal than the precipitation with carbonate in the manure biochar (68% vs 32%), while the contribution of the precipitation with carbonate in the straw biochar was more evident (64% vs 36%). This study first quantified the contribution of different biochar fractions to the Pb(II) removal and found that the inorganic fractions play the dominant role in the Pb(II) removal by biochar.

Keywords: Biochar; Inorganic minerals; Organic carbon; Precipitation; Sorption

Introduction

Biochar, usually generated from incomplete pyrolysis of carbon-rich materials, has received considerable interest as a recalcitrant carbon stock and consequently as a soil amendment to improve soil fertility, crop production, and nutrient retention [1-4]. Recently, biochar is also regarded as a promising low-cost biosorbent for heavy metals [2, 4-7] due to its abundance of organic functional groups as well as inorganic minerals [8, 9]. Activated carbon-like structure such as high surface area and porosity may also contribute to biochar's sorption ability [4, 10].

Many studies indicated the role of organic functional groups in biochar for heavy metal removal. Jiang et al [11] and Tong et al [12] showed that Pb or Cu sorption by biochar was mainly through the formation of surface complexes between metal and -COOH or -OH groups. Uchimiya et al [13] pointed out that biochars rich in -COOH groups exhibited significantly greater Pb, Cu, and Zn stabilization ability. The sorption of heavy metals on the functional groups such as -COOH, alcoholic-OH or phenolic-OH groups may involve electrostatic attraction and inner-sphere surface complex [14].

In addition to the richness of functional group-containing organic carbon, biochar often contain high levels of inorganic components such as alkali or alkaline earth metals (such as Ca, Mg, K, Na) which are often in the form of carbonates, phosphates or oxides [15]. All these inorganic components show contributions to the heavy metal removal to some extents [14]. Inyang et al [16] showed that sorption of Pb onto biochar was at least partly related to the Pb precipitation with the biochar minerals though the surface sorption was the principal mechanism. Jiang et al [17] showed that effective immobilization of Cu by biochar was partly attributed to alkaline substances such as CO_3^{2-} although oxygen-containing functional groups played a greater role than alkalinity.

Most of the studies indicate that heavy metal removal by biochar was the combined effect of its organic and inorganic fractions [9, 15, 18]. However, the interactions of each fraction with metals and quantification of their contribution to the metal sorption are not understood. Our previous work demonstrated that inorganic components such as CO_3^{2-} and PO_4^{3-} played an important role in the sorption of heavy metals by biochar derived from diary manure while the role of organic functional groups was pretty small [19, 20]. In this study, we took the further attempts: First separated inorganic and organic fractions from the dairy

manure biochar, then elucidated the interaction of each fraction with Pb, and last quantified the contribution of each fraction to the Pb sorption. For comparison, the biochar produced from rice straw was included in this work.

Materials and methods

Preparation and characterization of biochar and its organic and inorganic fractions

The biochars used in this study were obtained from two waste biomasses, dairy manure and rice straw, through a slow pyrolysis process. The details on biochar preparation have been described previously [15]. Briefly, the dried dairy manure and rice straw were ground to pass through a 2-mm sieve and heated at 500 °C for 4 h in a stainless steel reactor in a Muffle Furnace under the O_2-limited condition. The residue left in the reactor after heating was C-rich solid and called as biochar [21]. The biochars derived from dairy manure and rice straw were referred to as DM-biochar and RS-biochar, respectively. To obtain inorganic minerals, about 0.5g biochar was put in an open crucible and heated at 500°C for 6h in the atmosphere in the Muffle Furnace to reduce the carbon fraction [22]. The products resulted from DM-biochar and RS-biochar were considered to be inorganic minerals and referred to as DM-inorganic and RS-inorganic, respectively. Due to the same temperature of 500°C used in both inorganic minerals separation and biochar production, the inorganic minerals were not supposed to change a lot during the separation process [22]. In order to separate organic fraction, about 2 g biochar was treated in 10 mL of mixed HCl+HF (0.1M:0.3M) solution four times, followed by thorough washing with distilled water four times to remove soluble salts and silicon [23]. The products resulted from DM-biochar and RS-biochar were considered to be organic fractions and referred to as DM-organic and RS-organic, respectively. The resulted biochars and their organic and inorganic fractions were ground to pass through a 0.2-mm sieve for later characterization and sorption experiment.

The concentrations of C and N in biochar and its organic and inorganic fractions were determined using the CHNS/O Analyzer (Perkin Elmer, 2400 II). The pH of biochar and its each fraction was measured using the pH/Ion 510 Bench Meter. The surface area was detected by N_2 adsorption isotherms at 77 K using a Surface Area and Porosimetry Analyzer (Micromeritics Inc., USA). Water soluble PO_4^{3-}, Cl^-, SO_4^{2-}, and CO_3^{2-} were determined using ion chromatography (Waters 2690 Separations103 Module, Waters Corporation, USA) and water soluble Ca^{2+} and Mg^{2+} were measured by atomic absorption spectrophotometer (AAS) (novAA350, Jena, Germany). The surface organic functional groups present in the biochar and its organic fraction were identified by fourier transform infrared spectroscopy (FTIR) (IR Prestige 21 FTIR, Shimadzu, Japan). The inorganic phases of biochar and its inorganic fraction were were analyzed using XRD (D/max-2200/PC, Japan Rigaku Corporation).

Sorption test

The kinetic experiment of sorption was conducted in polypropylene tubes by mixing 0.125 g biochar (or each fraction) with 0.01M $NaNO_3$ solution containing 10 mM Pb(II). The pH of each mixed solution was adjusted to 5.5 with 0.1M HCl or NaOH solution through the whole sorption process. The pH was controlled at 5.5 because the initial pH values of all the mixed solutions were between 5 and 6. The mixed solutions were then shaken at 100 rpm and 5-mL solution was collected at the designated times. Each solution was centrifuged at 4,000 rpm for 15 min followed by filteration through a 0.22-μm Millipore filter. The filtrate was immediately acidified to pH< 2 with concentrated HNO_3 for Pb detection by AAS. The kinetic sorption curves were plotted by the sorption amount vs time.

The isotherm experiment of sorption was performed in 60-mL polypropylene tubes by mixing 0.125g biochar (or each fraction) with 0.01M $NaNO_3$ solution containing 0-10 mM Pb(II). For the similar reason to that in the kinetic experiment above, the pH of each mixed solution was adjusted to 5.5 with 0.1M HCl or NaOH solution through the whole sorption process. The mixed solutions were then shaken at 100 rpm until the equilibrium was reached. This took within 24h determined by the kinetic test (data shown below). After equilibrium, solid and liquid phases were separated and filtered as that in the kinetic experiment. The filtrate was immediately acidified for determination of Pb(II) by AAS. The isotherm sorption curves were plotted by the sorption amount vs Pb equilibrium concentrations. The solids were washed free of Pb(II) using 0.01M $NaNO_3$ followed by de-ionized H_2O and characterized by XRD and FTIR.

Modelling of heavy metal speciation

For simplicity, only one Pb(II) concentration, i.e., 8mM for biochar, 10 mM for inorganic fraction, and 0.1mM for organic fraction, was chosen for the speciation modeling. The different concentrations of Pb(II) were selected for different sorbents to allow for the maximum sorption being reached according to the sorption experiment above. Twenty five mL of 0.01 M $NaNO_3$ solution containing Pb(II) and biochar (or each fraction) was shaken to reach equilibrium. The pH of each mixed solution was adjusted to 5.5 with 0.1M HCl or NaOH solution through the whole sorption process. After equilibrium, separation of solid and liquid phases was conducted as done as in the sorption test section above. Half of the filtrate was collected for dissolved organic C (DOC) measurement using organic C analyzer (TOC-V/SSM-5000, Shimadzu, Japan) and for anions (PO_4^{3-}, SO_4^{2-}, Cl^-, NO_3^-, and CO_3^{2-}) analysis using ion chromatography. Remaining filtrate was acidified to pH<2 with HNO_3 for determination of cations (Pb, Ca, Mg, Fe, Al, Mn, Na, and K) using AAS. All analytical results including pH, DOC, anions, and cations were input in the Visual MINTEQ model [24] to calculate metal species in both solid and liquid phases.

Quality control

All experiments were conducted in triplicates at room temperature and included three controls: 0.01M $NaNO_3$ solution only, Pb(II) solution only, and biochar (or each fraction) + 0.01M $NaNO_3$ solution. Sorption of Pb(II) was calculated from the difference between initial and final solution concentrations after taking controls into account. Actually, the control effect was much less and can be negligible. The data presented in Tables and Figures were the average of the three replicates.

Results and discussion

Characterization of biochar and its organic and inorganic fractions

The selected properties of the dairy manure- and rice straw-derived biochars and their corresponding organic and inorganic fractions are listed in Table 1. Organic fraction was in major proportion (greater than 60%) in both DM and RS biochars compared with the inorganic fraction (less than 40%). Results indicated that both biochars are a complex of organic and inorganic components, which is in accordance to the previous work [25]. Rice straw is rich in hemicelluloses and celluloses [26], so RS-biochar contained more C than DM-biochar (57.2% vs 44.7%). Washing biochar with a mixture of HCl and HF acid dramatically increased C in the DM- and RS-organic fractions to 70.4 % and 75.9%, respectively. Correspondingly, more than 93% of Ca and Mg and nearly 100% of CO_3^{2-} and PO_4^{3-} were removed from the biochars. The XRD further evidenced the disappearance of peaks for $CaCO_3$ ($2\theta=29.5^o$) and $Ca_3(PO_4)_2$ ($2\theta=31^o$) in DM and RS organic fractions, compared with the DM and RS biochars (Fig. 1). These observations again demonstrated that the acid washing method could efficiently remove the inorganic fractions from biochar [23, 27].

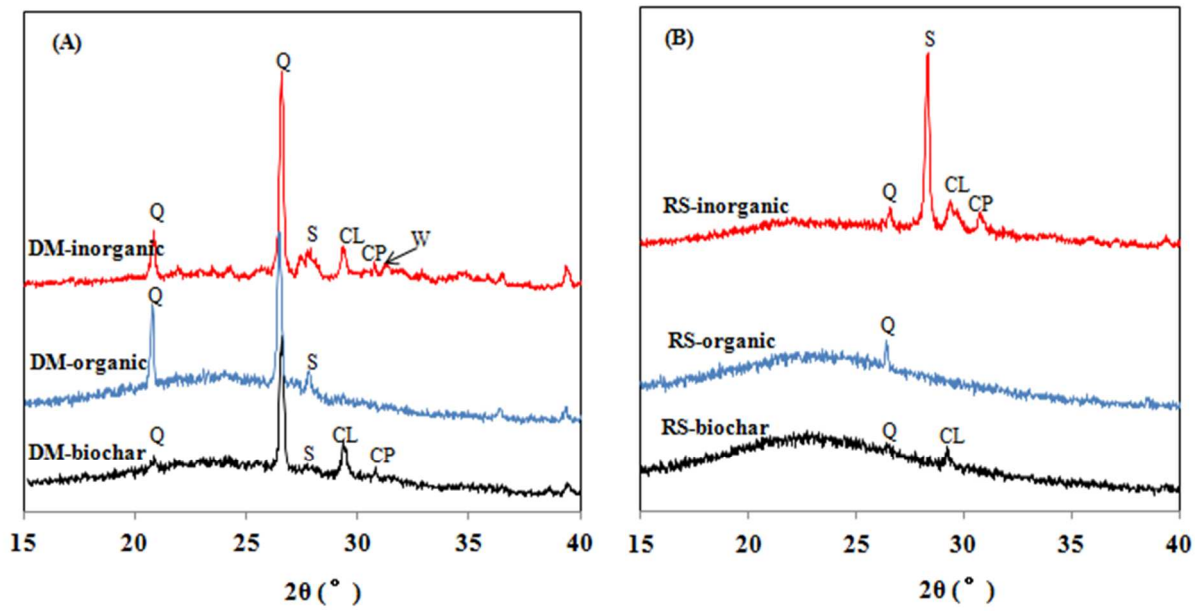

Fig.1 XRD patterns of (A) DM biochar and its components and (B) RS biochar and its components. Q, SiO_2; CL, $CaCO_3$; CP, $Ca_3(PO_4)_2$; W, $(Mg, Ca)_3(PO_4)_2$; S, KCl.

Table 1 Selected properties and elemental composition of biochar and its organic and inorganic fractions

	Fraction in biochar (%)	pH	Surface area ($m^2\ g^{-1}$)	TC (%)	TN (%)	PO_4^{3-}	Cl^-	CO_3^{2-}	SO_4^{2-}	Ca^{2+}	Mg^{2+}
						mg g^{-1}					
DM-biochar		10.2	150	44.7	1.99	28.2	17.1	9.44	5.92	21.7	7.60
DM-organic	61.4	3.74	264	70.4	1.59	-[a]	3.58	-	0.55	1.45	0.13
DM-inorganic	38.6	10.4	84.1	1.33	2.75	86.1	48.8	13.9	42.0	62.0	29.0
RS-biochar		9.78	128	57.2	1.58	8.06	16.06	10.0	4.17	9.59	2.29
RS-organic	68.9	3.66	302	75.9	0.07	-	2.07	-	0.46	0.59	0.047
RS-inorganic	31.1	10.7	56.2	1.24	1.59	34.7	57.0	17.3	27.8	50.1	15.4

[a] Below detection limit

To obtain inorganic fraction, the biochars were heated at 500°C in the atmosphere, which reduced total C from 44.7% in DM-biochar to1.33 % in DM-inorganic and from 57.2% in RS-biochar to 1.24% in RS-inorganic, with more than 97% of C in both biochars removed during the separation process (Table 1). XRD analysis (Fig.1) showed the disappearance of noncrystalline C peak between $2\theta=15\text{-}30^o$ [27] in the RS-inorganic and DM-inorganic which existed in the biochars and biochar organic fractions. Contrary to C, the contents of inorganic elements such as cations (Ca, Mg) and anions (PO_4^{3-}, Cl^-, CO_3^{2-}, SO_4^{2-}) increased dramatically (Table 1), resulting in the appearance of some new peaks in XRD patterns of inorganic fractions compared to the biochars. Increase of Ca, Mg, and P coupled with C decrease allowed the appearance of $(Mg,Ca)_3(PO_4)_2$ ($2\theta=31\text{-}33^o$) in DM-inorganic and $Ca_3(PO_4)_2$ in RS-inorganic which were not found in both biochars (Fig.1). The peak of $CaCO_3$ was enhanced in inorganic fractions of both biochars due to the elevated Ca and CO_3^{2-} concentrations. The new peak of KCl ($2\theta=28^o$) appeared in DM-inorganic and RS-inorganic (Fig.1) due to the increased Cl content in the inorganic fractions compared to their biochars (Table 1). These observations indicated the thermal treatment method could efficiently remove the organic fractions from biochar [22].

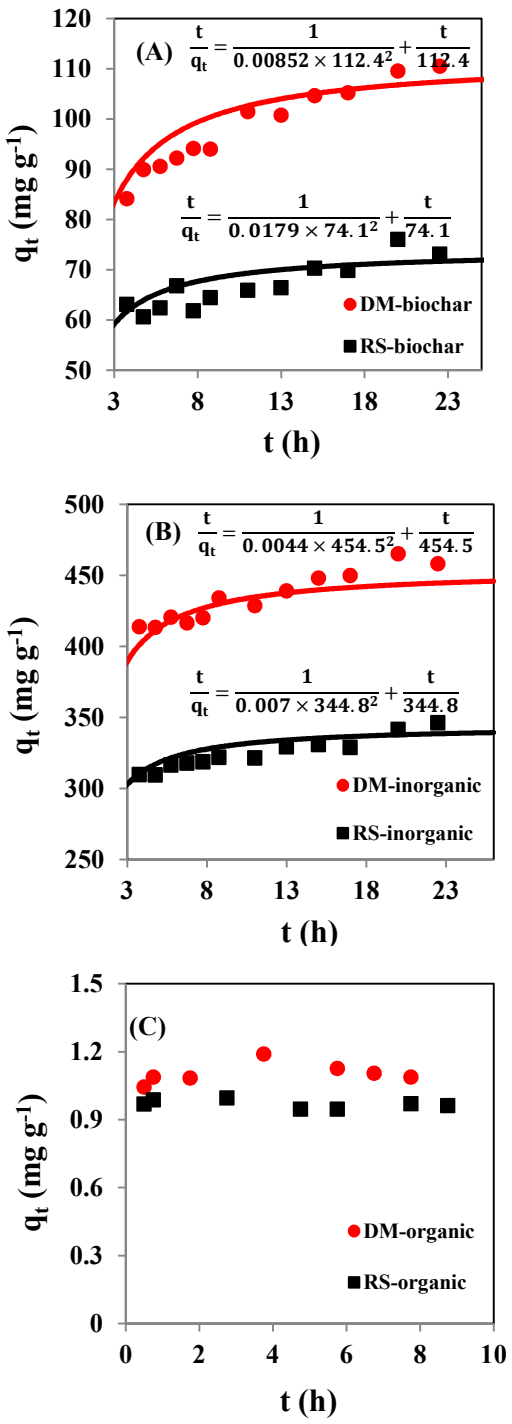

Fig.2 Kinetic study of Pb^{2+} sorption by (A) biochars, (B) biochar inorganic fractions and (C) biochar organic fractions, fitted with the pseudo-second order model.

The surface area of the organic fractions was about double that of their corresponding biochars. On the contrary, the surface area of the inorganic fraction decreased dramatically and was only about half of that of their biochars (Table 1). Therefore, the organic fraction contributed the major part to the biochar surface area. The pH of inorganic fractions increased, compared with those of the corresponding biochars (Table 1). The increase in pH was partly due to elevated CO_3^{2-} content, agreeing with the observation of Yuan [28]. The pH of organic fractions was reduced to below 4, much lower than that of the biochars, partly attributed to the acid washing treatment for the separation.

Sorption of Pb by biochar and its organic and inorganic fractions

The kinetics of Pb(II) sorption by the two biochars and their inorganic fractions could be well described by the pseudo-second order model

$$\frac{t}{q_t}=\frac{1}{q_e^2 k_1}+\frac{t}{q_e}$$

Where k_1 is the rate constant (min^{-1}), q_t is the amount of sorbed Pb(II) at t time (mg g^{-1}), and q_e is the amount of sorbed Pb(II) at equilibrium (mg g^{-1}).

The rate constant k_1 in both biochars (0.018 for RS-biochar and 0.008 for DM-biochar) were higher than their corresponding inorganic fractions (0.007 for RS-inorganic and 0.004 for DM-inorganic) (Fig. 2A and B), indicating a faster Pb(II) sorption by biochars. This was probably due to a relatively lower contribution of the rate-limited chemisorptions such as precipitation in the biochar [14], compared to that in the inorganic fractions. Nevertheless, the sorption of Pb(II) by RS-biochar and RS-inorganic almost reached equilibrium after 10 h, while the sorption equilibrium for those of dairy manure took a longer time, about 15 h (Fig. 2A and B). The long equilibration time for both biochar and their inorganic fractions may be attributed to their mesoporous properties, which had a pore size of 3.34-3.75 nm [25]. This is consistent with adsorption kinetics on activated carbon, as reported by Peel and Benedek [29]. However, a reverse order was obtained for the amount of Pb(II) sorbed (q_e) at equilibrium—DM-biochar and its inorganic fraction had higher q_e than those of RS-biochar and RS-inorganic (Fig. 2A and B). It seemed that Pb(II) reacted with the functional groups or minerals in the DM-biochar but not with all of them in the RS-biochar and its inorganic fraction [30]. This probably explained the reverse affinity orders obtained from k_1 and q_e analyses.

The kinetics of Pb(II) sorption by organic fractions failed to be fitted by any model. Actually, the sorption was rapid and completed within a few hours (Fig. 2C). It suggested that electrostatic adsorption, which is commonly considered to reach equilibrium in few minutes [31], may contribute to Pb(II) sorption by the organic fraction of biochar. Limited sorption capacity of organic fraction for Pb may also contribute to the fast sorption process.

The isotherms of Pb(II) sorption by RS-biochar and both two biochar organic fractions were of L-type according to the classification of Giles and Smith [32], while the isotherms of Pb(II) sorption by DM-biochar and both two biochar inorganic fractions

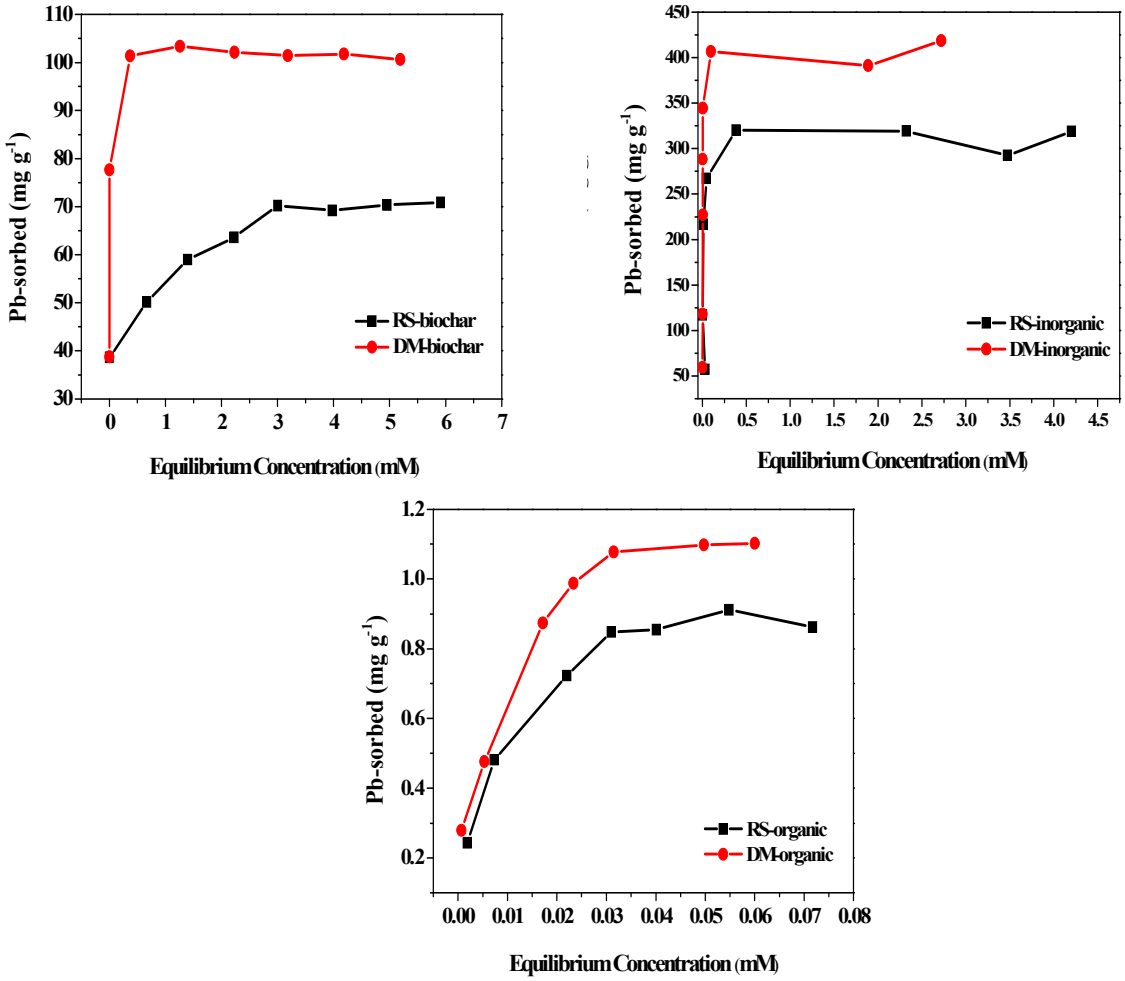

Fig. 3 Isotherms of Pb sorption by (A) biochars, (B) biochar inorganic fractions and (C) biochar organic fractions.

Table 2 Comparison of removal percentage of heavy metals by the biochar and its organic and inorganic fractions with the precipitation percentage of heavy metals predicted by Visual MINTEQ model (Electrolyte: 0.01 M $NaNO_3$ Pb=8mM for biochars , 10 mM for inorganic fraction and 0.1mM for organic fraction)

	Pb removal determined (%)	Pb precipitation predicted (%)	Pb precipitation/Pb removal (%)	Each Pb precipitate species in whole precipitation	
				$Pb_5(PO_4)_3Cl$ (%)	$Pb_3(CO_3)_2(OH)_2$ (%)
DM-biochar	31.9	47.7	100	68.0	32.0
DM-organic	34.2	-[a]	-	-	-
DM-inorganic	71.2	65.2	91.6	81.7	18.3
RS-biochar	29.1	26.1	89.7	36.3	63.7
RS-organic	22.5	-	-	-	-
RS-inorganic	55.0	37.1	67.5	58.7	41.3

[a] Below detection limit

were of H-type where the adsorbate-substrate affinity is especially high (Fig. 3). In fact, sorption of Pb(II) by inorganic minerals was a vertical line in which equilibrium concentrations were at the detection limit of the analytical method employed over the initial concentrations ranging from 0 to 5 mM. Isotherms that have similar equilibrium concentrations for different amounts of metal added reflect a precipitation mechanism [33].

XRD analysis of both DM-biochar and RS-biochar after Pb(II) sorption showed new peaks of $PbCO_3$ (2θ=24.8-25.2°), $Pb_3(CO_3)_2(OH)_2$ (2θ=24.8°, 34.5°), and $Pb_5(PO_4)_3Cl$ (2θ=26.5°, 29-32°), compared with the their original biochar (Fig. 4A and B). It indicated that precipitation of Pb(II) with carbonate and phosphate played an important role in the Pb(II) removal. Visual MINTEQ modeling further evidenced that 100% of Pb(II)

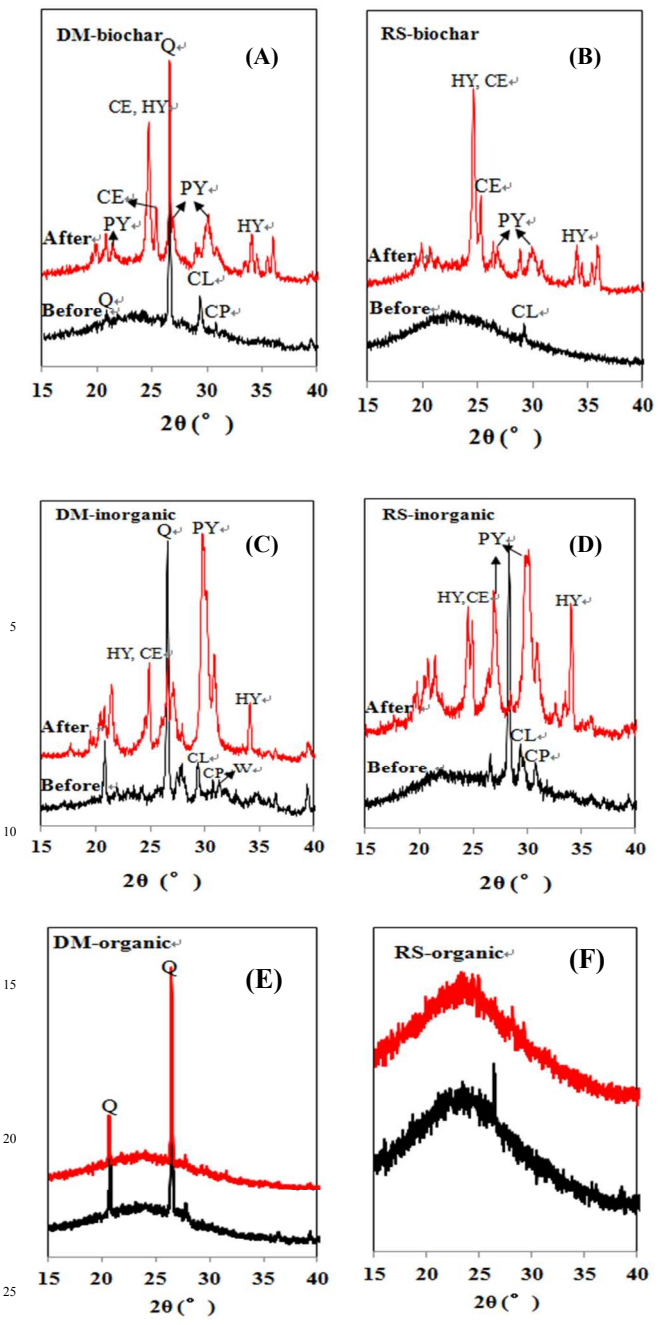

Fig. 4 XRD patterns of biochar and its organic and inorganic fractions before and after Pb sorption. Minerals with peaks labeled: PY, $Pb_5(PO_4)_3Cl$; CE, $PbCO_3$; HY, $Pb_3(CO_3)_2(OH)_2$; Q, SiO_2; CL, $CaCO_3$; CP , $Ca_3(PO_4)_2$.

removal by DM-biochar and 90% of that by RS-biochar was attributed to the precipitation of Pb(II) phosphates and Pb carbonates when the initial Pb(II) concentration was 8mM. Among precipitation in DM-biochar, 68% resulted from phosphate precipitates and 32% from carbonate precipitates while in RS-biochar the carbonate precipitates were the major product, accounting for 64% of the total precipitates (Table 2). DM-inorganic and RS-inorganic after Pb(II) sorption showed the same new peaks of carbonate and phosphate precipitation as their corresponding Pb-sorbed biochars (Fig. 4C and D). The difference is that DM-inorganic and RS-inorganic had higher peak intensity than their biochars, due to the higher PO_4^{3-} and CO_3^{2-} in inorganic fractions, compared to those in their biochars (Table 1). Organic functional groups such as carboxyl groups present in the biochar could form strong complexes with aqueous Pb(II) [34]. This would probably inhibit formation of Pb phosphate and carbonates, resulting in relatively lower peak intensity.

The Visual MINTEQ modeling showed that the precipitation accounted for 91.6% of Pb(II) removal by DM-inorganic and 67.5% of Pb(II) removal by RS-inorganic (Table 2). Among the precipitation, 81.7% of Pb precipitates in the exhausted DM-inorganic was in the form of $Pb_5(PO_4)_3Cl$ and 18.3% was in the form of $Pb_3(CO_3)_2(OH)_2$ (Table 2). For RS-inorganic, $Pb_5(PO_4)_3Cl$ and $Pb_3(CO_3)_2(OH)_2$ accounted for 58.7% and 41.3% of the Pb precipitates, respectively. In addition to the precipitation, there was still a fair amount of Pb(II) (8.4% and 32.5% for DM-inorganic and RS-inorganic, respectively, Table 2) which was removed probably through ion exchange or complexation [35].

For the organic fractions, XRD patterns (Fig. 4E and F) and FTIR spectrum (Fig. 5) remained unchanged before and after Pb(II) sorption. This was probably because the concentration of Pb(II) in the Pb(II)-exhausted samples was below the detection limits as the sorption capacities of both organic fractions were only around 1 mg g^{-1} (Fig. 3C). The FTIR spectra of the organic fraction samples shown in Fig. 5 had several bands, which were assigned to carboxylic acid -COOH or C=C (1550-1650 cm^{-1}) [36] and phenolic–OH (3200-3400 cm^{-1}) [8]. Phenolic–OH group usually has pKa values ranging from 7 to 10 or more [37], thus, the dissociation of protons from phenolic-OH is unlikely to happen in the tested pH (5.5). However, the -COOH group has pKa values of between 2 and 4 [38], it is likely dissociated at the tested pH (5.5) and hence expected to contribute to the Pb(II) removal by the organic fractions via either electrostatic attraction or/and inner-sphere surface complex [14]. The sorption of Pb(II) by organic fractions may also be associated with the electron-rich domains on functional groups bearing π-electrons such as C=O or C=C to form cation-π interactions [39].

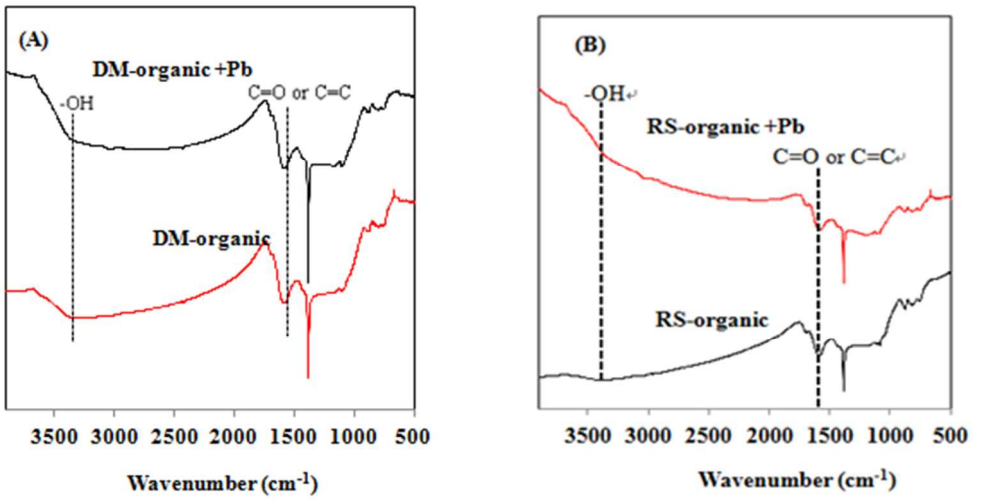

Fig.5 FTIR analysis of (A) DM-organic and (B) RS-organic before and after Pb sorption

Table 3 Contribution of organic and inorganic fractions to the Pb removal by biochars

	Fraction in biochar (%)	Determined capacity for Pb removal (mg g^{-1})	Calculated capacity normalized into biochar (mg g^{-1})	Fractional Pb removal/total Pb removal by biochar (%)
DM-biochar		110	159	
DM-organic	61.4	1.10	0.68	0.40
DM-inorganic	38.6	410	158	99.6
RS-biochar		71.5	100	
RS-organic	68.9	0.90	0.62	0.60
RS-inorganic	31.1	320	99.5	99.4

Contribution of the organic and inorganic fractions to the sorption of Pb by biochars

As shown in Fig. 3, inorganic minerals showed higher affinity for Pb(II) than biochars. The sorption capacities of Pb(II) by RS-inorganic and DM-inorganic were over 300 mg g^{-1}, much higher than those of biochars (below 110 mg g^{-1}) (Fig. 3 and Table 3). However, the maximum sorption capacity of Pb(II) by the two biochar organic fractions was much less and only about 1 mg g^{-1} (Fig.3). The results indicated that inorganic minerals in the biochars were mainly responsible for the high sorption ability of biochars, in accordance to our previous observation [19, 20].

In order to quantify the contribution of biochar organic and inorganic fractions to the Pb(II) removal, a calculation was conducted by normalizing Pb(II) sorption by each fraction into that by the whole biochar. The results showed that DM-organic and RS-organic accounted for 0.4% and 0.6% in DM and RS biochars, respectively, whereas biochar inorganic fractions, i.e., DM-inorganic and RS-inorganic, were responsible for over 99% of Pb(II) removal by the total biochars (Table 3). Note that the calculated sorption capacities of DM-biochar and RS-biochar by summing organic and inorganic fraction were 159 mg g^{-1} and 100 mg g^{-1}, respectively, larger than the experimental data (101 mg g^{-1} for DM-biochar and 70 mg g^{-1} for RS-biochar) (Fig. 3). The discrepancy may be due to the complexity of Pb(II) sorption to the biochars which inhibited each organic and inorganic fractions act sufficiently.

Conclusions

The results from this study showed that biochar organic and inorganic fractions contribute to the Pb(II) removal to a different extent and follow the different mechanisms. Though lots of work has proved that biochar is a promising sorbent for the heavy metals, less work took further efforts to determine the contribution of main components in biochar to the metal removal. Our study made the first quantification and determined that the inorganic fractions in biochar play the dominant role in the Pb(II) sorption. These further attempts have a great implication for our understanding how the biochar simultaneously functions as sorbent for immobilization of heavy metals while biochar is applied into soil as carbon sequestration pool. Our work further indicated that sorption of Pb(II) by the organic fraction was probably through the intrinsic chemical affinity with –COO-, and/or cation-π interactions, while the inorganic fraction sorbed Pb(II) via the chemisorption, primarily through the inner-sphere complexation and precipitation.

Acknowledgements

This work was supported in part by National Natural Science Foundation of China (No. 21107070, 21377081), Shanghai Science and Technology Commission (13231202502), and Shanghai Education Commission (14ZZ026), and Shanghai Environmental Protection Bureau (Huhuanke2013-04).

Notes and references

[a] *School of Environmental Science and Engineering, Shanghai Jiao Tong University, 800 Dongchuan Road, Shanghai 200240, China. Tel: +86 21 3420 2841; E-mail: xdcao@sjtu.edu.cn*

[b] *Shanghai Academy of Environmental Sciences, 508 Qinzhou Road, Shanghai 200233, China.*

1. J. Lehmann, *Nature*, 2007, **447**, 143-144.
2. L. Beesley, E. Moreno-Jimenez, J. L. Gomez-Eyles, E. Harris, B. Robinson and T. Sizmur, *Environmental Pollution*, 2011, **159**, 3269-3282.
3. J. Lehmann, J. M. Kimetu, S. O. Ngoze, D. N. Mugendi, J. M. Kinyangi, S. Riha, L. Verchot, J. W. Recha and A. N. Pell, *Ecosystems*, 2008, **11**, 726-739.
4. X. C. Chen, G. C. Chen, L. G. Chen, Y. X. Chen, J. Lehmann, M. B. McBride and A. G. Hay, *Bioresource Technology*, 2011, **102**, 8877-8884.
5. Y. Qiu, H. Cheng, C. Xu and G. D. Sheng, *Water Research*, 2008, **42**, 567-574.
6. L. Beesley, E. Moreno-Jimenez and J. L. Gomez-Eyles, *Environmenntal Pollution*, 2010, **158**, 2282-2287.
7. M. Ahmad, A. U. Rajapaksha, J. E. Lim, M. Zhang, N. Bolan, D. Mohan, M. Vithanage, S. S. Lee and Y. S. Ok, *Chemosphere*, 2014, **99**, 19-33.
8. M. Uchimiya, I. M. Lima, K. T. Klasson, S. C. Chang, L. H. Wartelle and J. E. Rodgers, *Journal of Agricultural and Food Chemistry*, 2010, **58**, 5538-5544.
9. X. D. Cao, L. N. Ma, B. Gao and W. Harris, *Environmental Science & Technology*, 2009, **43**, 3285-3291.
10. L. Beesley and N. Dickinson, *Soil Biol Biochem*, 2011, **43**, 188-196.
11. T. Y. Jiang, J. Jiang, R. K. Xu and Z. Li, *Chemosphere*, 2012, **89**, 249-256.
12. X. Tong, J. Li, J. Yuan and R. Xu, *Chemical Engineering Journal*, 2011, **172**, 828-834.
13. M. Uchimiya, D. I. Bannon and L. H. Wartelle, *Journal of Agricultural and Food Chemistry*, 2012, **60**, 1798-1809.
14. H. L. Lu, W. H. Zhang, Y. X. Yang, X. F. Huang, S. Z. Wang and R. L. Qiu, *Water Research*, 2012, **46**, 854-862.
15. X. D. Cao and W. Harris, *Bioresource Technology*, 2010, **101**, 5222-5228.
16. M. Inyang, B. Gao, W. Ding, P. Pullammanappallil, A. R. Zimmerman and X. Cao, *Separation Science and Technology*, 2011, **46**, 1950-1956.
17. J. Jiang and R. K. Xu, *Bioresource Technology*, 2013, **133**, 537-545.
18. N. Karami, R. Clemente, E. Moreno-Jimenez, N. W. Lepp and L. Beesley, *Journal of Hazard Material*, 2011, **191**, 41-48.
19. X. Xu, X. Cao, L. Zhao, H. Wang, H. Yu and B. Gao, *Environmental Science and Pollution Research*, 2013, **20**, 358-368.
20. X. Xu, X. Cao and L. Zhao, *Chemosphere*, 2013, **92**, 955-961.
21. J. Lehmann, *Frontiers in Ecology and Environment*, 2007, **5**, 381-387.
22. T. A. J. Kuhlbusch, *Environmental Science & Technology*, 1995, **29**, 2695-2702.
23. Y. Yang and G. Sheng, *Environmental Science & Technology*, 2003, **37**, 3635-3639.
24. J. P. Gustafsson, 2010.
25. L. Zhao, Zheng, W., Cao, X.D., *Chemical Engineering Journal*, 2014.
26. B. Xiao, X. F. Sun and R. C. Sun, *Polymer Degradation and Stability*, 2001, **74**, 307-319.
27. M. Xie, W. Chen, Z. Xu, S. Zheng and D. Zhu, *Environmental Pollution*, 2014, **186**, 187-194.
28. J. H. Yuan, R. K. Xu and H. Zhang, *Bioresource Technology*, 2011, **102**, 3488-3497.
29. R. G. B. Peel, A., *Journal of Environmental Engineering-ASCE*, 1980, **106** 797-813.
30. Z. Reddad, C. Gerente, Y. Andres and P. Le Cloirec, *Environmental Science & Technology*, 2002, **36**, 2067-2073.
31. W. Zhang and I. Lo, *Journal of Environmental Engineering*, 2006, **132**, 1282-1288.
32. C. H. Giles, D. Smith and A. Huitson, *Journal of Colloid and Interface Science*, 1974, **47**, 755-765.
33. X. Cao, L. Q. Ma, D. R. Rhue and C. S. Appel, *Environmental Pollution*, 2004, **131**, 435-444.
34. R. A. Berner, *American journal of science (1880)*, 1978, **278**, 816-837.
35. X. B. Chen, J. V. Wright, J. L. Conca and L. M. Peurrung, *Environmental Science & Technology*, 1997, **31**, 624-631.
36. J. Zhu, B. Deng, J. Yang and D. Gang, *Carbon*, 2009, **47**, 2014-2025.
37. M. D. Liptak, K. C. Gross, P. G. Seybold, S. Feldgus and G. C. Shields, *Journal of the American Chemical Society*, 2002, **124**, 6421-6427.
38. D. M. Barkauskas Jurgis, *Journal of the Serbian Chemical Society*, 2004, **69**, 363-375.
39. O. R. Harvey, B. E. Herbert, R. D. Rhue and L.-J. Kuo, *Environmental Science & Technology*, 2011, **45**, 5550-5556.